

Imaging of C-X-C Motif Chemokine Receptor 4 Expression in 690 Patients with Solid or Hematologic Neoplasms using ⁶⁸Ga-PentixaFor PET

Andreas K. Buck^{1,*}, Alexander Haug^{2,*}, Niklas Dreher¹, Alessandro Lambertini¹, Takahiro Higuchi^{1,3}, Constantin Lapa⁴, Alexander Weich⁵, Martin G. Pomper⁶, Hans-Jürgen Wester⁷, Anja Zehndner^{1,8}, Andreas Schirbel¹, Samuel Samnick¹, Marcus Hacker², Verena Pichler⁹, Stefanie Hahner¹⁰, Martin Fassnacht¹⁰, Hermann Einsele¹¹, Sebastian E. Serfling^{1,#}, Rudolf A. Werner^{1,6#}

¹ Department of Nuclear Medicine, University Hospital Würzburg, Germany;

² Division of Nuclear Medicine, Medical University of Vienna, Vienna, Austria;

³ Okayama University Graduate School of Medicine, Dentistry and Pharmaceutical Sciences, Okayama, Japan;

⁴ Nuclear Medicine, Medical Faculty, University of Augsburg, Germany;

⁵ Department of Internal Medicine II, Gastroenterology and ENETS Center of Excellence, University Hospital Würzburg, Germany;

⁶ The Russell H Morgan Department of Radiology and Radiological Sciences, Johns Hopkins School of Medicine, Baltimore, MD;

⁷ Pharmaceutical Radiochemistry, Technische Universität München, München, Germany;

⁸ Pentixapharm Würzburg, Würzburg, Germany;

⁹ Division for Pharmaceutical Chemistry, Medical University of Vienna, Vienna, Austria;

¹⁰ Division of Endocrinology and Diabetes, Department of Medicine I, University Hospital, University of Würzburg, Germany;

¹¹ Department of Internal Medicine II, Hematology and Oncology, University Hospital Würzburg, Würzburg, Germany.

*,# equally contributed.

Brief Title: ⁶⁸Ga-PentixaFor in 690 patients

Word Count: 3,934

Address for Correspondence:

Andreas K. Buck, MD

Department of Nuclear Medicine

University Hospital Würzburg

Oberdürrbacher Str. 6

97080 Würzburg

Mail: buck_a@ukw.de

Phone: +49 931 201 35000

Fax: +49 931 201 35001

ABSTRACT

Background: In recent years, molecular imaging addressing the C-X-C motif chemokine receptor 4 (CXCR4) has increasingly been utilized in various clinical settings. Here, we aimed to assess radiopharmaceutical uptake and image contrast to determine the most relevant clinical applications for CXCR4-directed imaging. We also investigated the impact of specific activity on scan contrast. **Methods:** 690 patients with a variety of neoplasms underwent a total of 777 PET/CT scans with ^{68}Ga -PentixaFor, serving as CXCR4-specific radioligand. A semiquantitative target lesion (TL) analysis was conducted [providing maximum standardized uptake values (SUV_{max}) and target-to-blood pool ratio (TBR), defined as SUV_{max} (from TL) divided by mean SUV (from blood pool)]. The applied specific activity (in $\text{MBq}/\mu\text{g}$) was compared to semi-quantitative assessments. **Results:** Of the 777 scans, 242 did not show discernible uptake in disease sites, leaving 535 PET scans (68.9%) for further analysis. Very high tracer uptake ($\text{SUV}_{\text{max}} > 12$) was found in multiple myeloma (MM; $n=113$), followed by adrenocortical carcinoma ($n=30$), mantle cell lymphoma (MCL; $n=20$), adrenocortical adenoma ($n=6$) and small cell lung cancer (SCLC; $n=12$). Providing information on image contrast, comparable results for TBR were recorded, with TBR (>8) in MM, MCL and acute lymphoblastoid leukemia ($n=6$). When comparing specific activity with semiquantitative parameters, no significant correlation was found for SUV_{max} or TBR ($P \geq 0.612$). **Conclusions:** In this large cohort, ^{68}Ga -PentixaFor demonstrated high image contrast in a variety of neoplasms, particularly for hematologic malignancies, SCLC and adrenocortical neoplasms. The present analysis may provide a roadmap to detect patients who may benefit from CXCR4-targeted therapies.

Keywords: CXCR4, C-X-C motif chemokine receptor 4, ^{68}Ga -PentixaFor, PET

INTRODUCTION

Due to its pivotal role in cancer progression, the C-X-C motif chemokine receptor 4 (CXCR4) orchestrates organ-specific tumor spread through several mechanisms. These include promotion of angiogenesis, growth of malignant cells or inhibition of antitumor immune response (1). Numerous CXCR4-directed molecular imaging agents have been developed recently to define precisely the utility of CXCR4 as an anti-cancer target (2-5). Among them, the ^{68}Ga -labeled radiotracer PentixaFor (cyclo(D-Tyr¹-D-[NMe]Orn²(AMBS- ^{68}Ga -DOTA)-Arg³-Nal⁴-Gly⁵) demonstrated high selectivity for CXCR4, along with rapid renal excretion (6,7). Accordingly, ^{68}Ga -PentixaFor has been utilized in a wide variety of clinical scenarios in oncology. These include patients with multiple myeloma (MM), marginal zone lymphoma or solid tumor entities, such as small- (SCLC) and non-small cell lung cancer, neuroendocrine neoplasms, and adrenocortical carcinoma (8-13). Of note, head-to-head comparison with established imaging modalities or other reference radiotracers revealed improved lesion detection rates by ^{68}Ga -PentixaFor PET (8,14,15). This may promote wider adoption of this imaging agent in patients for whom existing modalities are lacking. Furthermore, $^{177}\text{Lu}/^{90}\text{Y}$ -Pentixather, a therapeutic counterpart to target CXCR4, has been applied for targeted radionuclide therapies in hematologic malignancies, such as MM or diffuse large B cell lymphoma (16,17). Such theranostic approaches have not only demonstrated a favorable outcome (16,17), but also tolerable adverse effects, although stem cell support is mandatory (18).

The beneficial use of ^{68}Ga -PentixaFor PET/CT, along with its potential to identify patients eligible for treatment with β -particle emitters, favors wider clinical use. However, prior to widespread adoption or clinical development programs leading to market authorization, comprehensive characterization of its performance should be undertaken, including assessment of radiopharmaceutical uptake and image contrast among a broad spectrum of neoplasms. In our bicentric study, which enrolled the largest cohort of patients imaged with ^{68}Ga -PentixaFor PET/CT or PET/MR to date, we aimed to assess radiopharmaceutical accumulation and image contrast in

several cancers to determine the most relevant clinical applications. In addition, lower specific activity characterized by higher amounts of cold mass could hamper image interpretation (19), e.g., by an increasing occupation of the (sub)cellular target by non-radiolabeled components. Thus, we also investigated the impact of specific activity on quantification.

MATERIAL AND METHODS

Patient Population

Patients from two study sites were included (University of Würzburg and Medical University of Vienna). Parts of this cohort have been described before to determine the diagnostic usefulness of ^{68}Ga -PentixaFor PET/CT (7-9,11-14,20-26), without evaluation of image contrast (including impact of specific activity) or comparing uptake among all included diagnoses. Patients signed written informed consent prior to the examination. Given the retrospective character of this study, the local ethics committee waived the need for further approval (No. 20210726 02).

Radiotracer Synthesis

Following GMP, ^{68}Ga -PentixaFor was provided using a synthesis module (Scintomics, Fürstenfeldbruck, Germany) and disposable single-use cassette kits (ABX, Radeberg, Germany), as described previously (27). Peptide mass (in μg), activity (in MBq) and specific activity (in MBq/ μg) of injected ^{68}Ga -PentixaFor were recorded for each patient.

Imaging

^{68}Ga -PentixaFor PET was performed either on a Siemens Biograph mCT (64 and 128, Siemens Medical Solutions, Erlangen, Germany) or on a Siemens Biograph mMR (Siemens Healthcare GmbH, Erlangen, Germany). Whole-body scans (covering the vertex of the skull to the proximal thighs) were conducted 60 min after injection of ^{68}Ga -PentixaFor. We also performed low-dose CT scans for attenuation correction and anatomical co-registration (120 keV, 512 x 512

matrix, 5 mm slices, increment: 30 mm/s, pitch index 0.8, and rotation time: 0.5 s). PET images were reconstructed including corrections for CT-based attenuation, random events, and scatter. For MR, we applied an integrated radiofrequency coil including a multi-station protocol (slice thickness, 2 mm), as previously described (12,28).

Image Interpretation

All scans were performed for clinical or research purposes. As part of this study, all images were reanalyzed by readers that were blinded to respective clinical information. At Würzburg, image interpretation was performed as a single-reader analysis (either ND or AL), verified by an expert reader (RAW). At Vienna, an expert reader carried out the assessment (AH).

Semiquantitative Assessment. A target lesion (TL) assessment was carried out by investigating the visually most intense TL on PET. Three-dimensional volumes-of-interest (VOI) applying an isocontour threshold of 40% were placed on the TL, providing maximum standardized uptake values (SUV_{max}), SUV_{mean} and peak SUV (SUV_{peak}). A target-to-blood pool ratio (TBR) was derived by placing a VOI over the aortic arch. TBR was then provided by dividing SUV_{max} (of the TL) by SUV_{mean} (of the blood pool) (12).

Statistical Analysis

Statistical analysis was performed using GraphPad Prism Version 9.2.0 (GraphPad Prism Software, La Jolla, CA, USA). Descriptive results are displayed as mean \pm standard deviation (SD). Nonparametric Spearman's correlation coefficients were calculated to investigate associations between semi-quantitative parameters with specific activity (including an outlier correction using the ROUT-Method). A *P*-value of <0.05 was considered statistically significant.

RESULTS

Highest Uptake in Hematologic Malignancies, SCLC, and Adrenocortical Neoplasms

No adverse events were recorded after injection of ^{68}Ga -PentixaFor. 242/777 (31.1%) of the scans did not show discernible uptake, leaving 535/777 (68.9%) cases for further analysis (Table 1). As such, an overall number of 535 TL were investigated. Among all TL, SUV_{max} was 13.01 ± 10.01 and the corresponding TBR was 8.59 ± 15.98 . The highest average SUV_{max} (>12) was found in MM ($n=113$), followed by adrenocortical carcinoma ($n=30$), mantle cell lymphoma (MCL; $n=20$), adrenocortical adenoma ($n=6$) and SCLC ($n=12$; Figures 1, 2). The lowest average SUV_{max} (<6) was recorded in osteosarcoma ($n=1$), followed by bladder cancer ($n=1$), mediastinal tumor (not otherwise specified, $n=1$), head and neck cancer ($n=2$) and Ewing sarcoma ($n=1$; Figure 3). For SUV_{peak} , comparable results were achieved (Supplemental Figure 1). Moreover, high average TBR (>8) was recorded in MM, MCL and acute lymphoblastoid leukemia ($n=6$). Low average TBR (<4) was observed in head and neck cancer, colorectal cancer ($n=1$), osteosarcoma, Ewing sarcoma, bladder cancer, renal cell carcinoma ($n=1$) and mediastinal tumor (Figure 4).

No Relevant Impact of Specific Activity on Visual or Semiquantitative Assessment

Median injected peptide mass was 8.5 μg (range, 2.56 – 35.61 μg), injected activity was 143 MBq (range, 38 – 239 MBq) and specific activity was 15.39 MBq/ μg (range, 2.19 – 43.70 MBq/ μg). Comparing specific activity to semiquantitative parameters, only SUV_{mean} ($\rho = -0.138$, $P = 0.002$), but none of the other correlative indices reached significance (SUV_{max} , $\rho = 0.01$, $P = 0.832$; TBR, $\rho = 0.023$, $P = 0.612$; SUV_{peak} , $\rho = -0.087$, $P = 0.053$; Figure 5).

DISCUSSION

In the present bi-centric study investigating a large cohort imaged with ^{68}Ga -PentixaFor, discernible uptake in putative sites of disease was noted in >68% of the scans. Among neoplasms studied, we determined MM had the highest uptake (SUV), with adrenocortical carcinoma and mantle cell lymphoma closely following. Comparable results were recorded for image contrast (TBR). Specific activity had no impact on a semi-quantitative level, supporting the notion that an excellent read-out can be achieved, even after administration at low specific activities.

A growing body of evidence supports the clinical utility of CXCR4-targeted ^{68}Ga -PentixaFor PET/CT in a variety of disease entities, including hematologic malignancies (7,22) and solid tumors (29). Some of these studies also revealed that ^{68}Ga -PentixaFor provided an increased detection rate at sites of disease when compared to conventional imaging or other PET agents such as 2'-deoxy-2'- ^{18}F -fluoro-D-glucose or somatostatin receptor-directed radiopharmaceuticals, thereby indicating that this agent can image malignancies that lack a more suitable modality (15,23,26). Here we aimed to provide a precise cohort of neoplasms that exhibit high tracer avidity and excellent TBR. By investigating 690 patients suffering from 35 different types of cancer, we demonstrated that ^{68}Ga -PentixaFor PET exhibits the most intense uptake in hematologic malignancies, such as MM, MCL or acute lymphoblastoid leukemia. ^{68}Ga -PentixaFor PET did not perform as well in solid tumors. Nevertheless, a TBR > 4 was still achieved in certain cases, e.g., adrenal, SCLC, liver, ovarian, neuroendocrine neoplasms, or pancreatic cancer (Figure 4). We also checked whether low specific activity may have hampered image contrast (19), e.g., by an increasing occupancy of the target by carrier. However, we ruled out a relevant impact on a semiquantitative level (Figure 5). This is also in line with previous affinity studies, demonstrating that ^{68}Ga -PentixaFor completely interacts with the binding pocket of CXCR4 (30). Nonetheless, novel second-generation radiotracers based on *iodo*CPCR4 analogs with altered linker structure may further increase tumor retention (31).

Increased CXCR4 expression on the tumor cells has been tightly linked to poor outcome in hematologic malignancies and solid tumors (32,33), suggesting it as a viable therapeutic target. For example, the stromal cell derived factor 1 neutralizing agent Olaptosed pegol (NOX-A12) or the CXCR4 antagonist Plerixafor have each been used in patients with refractory MM. In clinical phase I/II studies, such drugs achieved an overall response rate in almost half of the patients (Plerixafor) or partial response in 68% (NOX-A12) (34,35). Theranostic approaches based on ^{68}Ga -PentixaFor scan results have also been conducted by using the therapeutic analogs $^{177}\text{Lu}/^{90}\text{Y}$ -Pentixather (16,18). Although there is no study reporting an association between PET-based SUV_{max} and absorbed doses in lesions upon CXCR4-directed imaging and radionuclides therapies to date, the markedly increased SUV_{max} observed in certain cases suggests that a substantial fraction of patients may also be eligible for CXCR4-directed radioligand therapies. However, CXCR4-targeted endoradiotherapy causes bone marrow ablation and, thus, subsequent stem cell support is needed (18), further emphasizing the importance of well-established algorithms for adequate patient selection.

Future studies should also evaluate the ability of CXCR4-directed molecular imaging to assess the retention capacities of non-radiolabeled CXCR4 neutralizing agents *in-vivo*, preferably prior to treatment onset. For instance, a phase I study evaluating the CXCR4 inhibitor LY2510924 in patients with advanced solid cancers revealed favorable antitumor activity (36). Of note, a substantial patient fraction treated with this “cold” CXCR4 inhibitor had the identical clinical diagnoses as in the present study, e.g., ovarian, lung or pancreatic cancer (all demonstrating $\text{SUV}_{\text{max}} > 6$). As such, a baseline ^{68}Ga -PentixaFor PET/CT revealing increased CXCR4 expression at disease sites may allow to identify patients that would most likely be suitable for non-radiolabeled CXCR4-directed drugs, including LY2510924 (36). This would then further expand

the theranostic concept beyond identifying patients for treatment with β -emitters, but also to select individuals for non-radiolabeled CXCR4-targeted therapeutic options.

Our study has several limitations. We included both CT- and MR-based hybrid imaging, which may provide an additional variable that could be controlled better in future studies. Despite investigating the largest cohort to date, prospective trials should also be undertaken. In addition, the numbers of investigated patients per tumor entity substantially varied. Thus, resulting low numbers of cases and inter- and intra-patient heterogeneity of in-vivo CXCR4 expression may have biased the herein presented results. Future studies should therefore consider more balanced subgroups enrolling comparable numbers of patients diagnosed with the identical tumor entity.

CONCLUSION

We found high uptake and image contrast for a variety of neoplasms imaged with ^{68}Ga -PentixaFor PET, such as MM and mantle cell lymphoma, but also for adrenal neoplasms and SCLC. These results suggest clinical scenarios in which ^{68}Ga -PentixaFor PET may prove beneficial for directing CXCR4-targeted therapies.

DISCLOSURES

H.J.W. is founder and shareholder of Scintomics. A.Z. is an employee of Pentixapharm, Würzburg. All other authors declare that there is no conflict of interest as well as consent for scientific analysis and publication.

KEY POINTS

QUESTION: What is the tracer avidity of malignant lesions and what are the most avid tumors for CXCR4-targeted ⁶⁸Ga-PentixaFor PET?

PERTINENT FINDINGS: We observed high uptake and image contrast of the radiopharmaceutical, in particular for hematologic malignancies as well as adrenal neoplasms and small cell lung cancer. Specific activity had no effect on ⁶⁸Ga-PentixaFor uptake.

IMPLICATIONS FOR PATIENT CARE: Among a broad spectrum of neoplasms, the present bicentric study suggests entities eligible for CXCR4-directed molecular imaging and therapy.

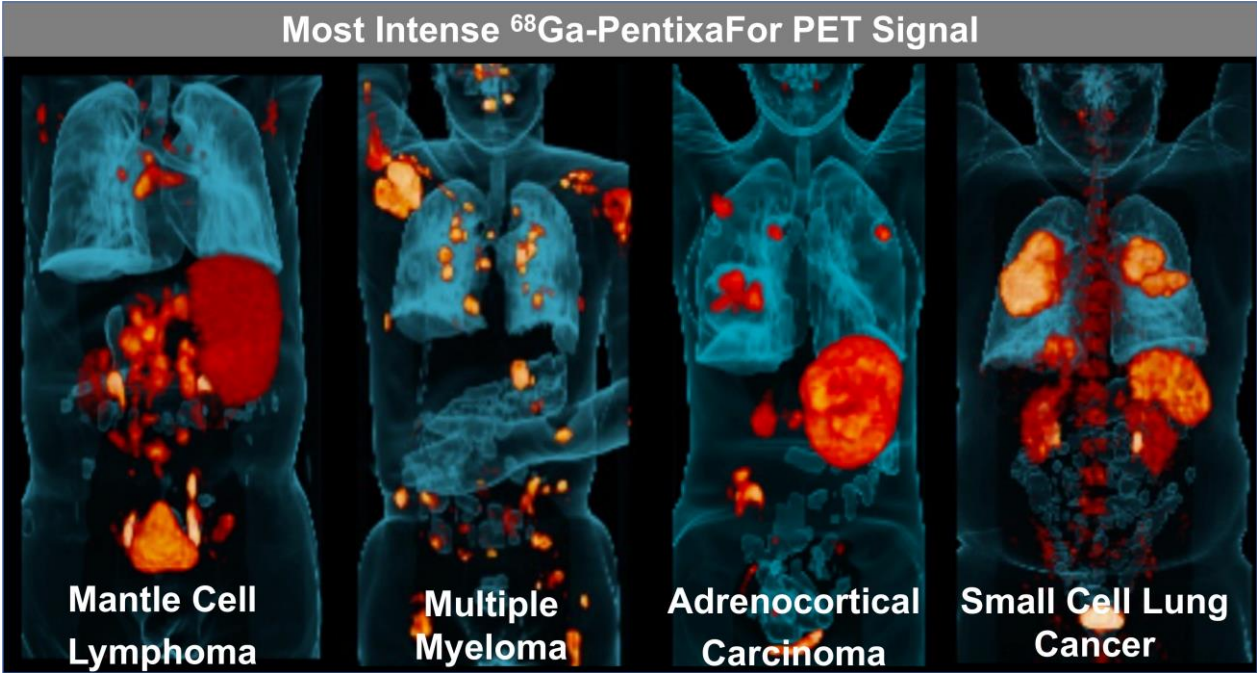
REFERENCES

1. Zlotnik A, Burkhardt AM, Homey B. Homeostatic chemokine receptors and organ-specific metastasis. *Nat Rev Immunol*. 2011;11:597-606.
2. Azad BB, Chatterjee S, Lesniak WG, et al. A fully human CXCR4 antibody demonstrates diagnostic utility and therapeutic efficacy in solid tumor xenografts. *Oncotarget*. 2016;7:12344-12358.
3. Nimmagadda S, Pullambhatla M, Stone K, Green G, Bhujwala ZM, Pomper MG. Molecular imaging of CXCR4 receptor expression in human cancer xenografts with [64Cu]AMD3100 positron emission tomography. *Cancer Res*. 2010;70:3935-3944.
4. De Silva RA, Peyre K, Pullambhatla M, Fox JJ, Pomper MG, Nimmagadda S. Imaging CXCR4 expression in human cancer xenografts: evaluation of monocyclam 64Cu-AMD3465. *J Nucl Med*. 2011;52:986-993.
5. Yan X, Niu G, Wang Z, et al. Al[18F]NOTA-T140 Peptide for Noninvasive Visualization of CXCR4 Expression. *Mol Imaging Biol*. 2016;18:135-142.
6. Demmer O, Gourni E, Schumacher U, Kessler H, Wester HJ. PET imaging of CXCR4 receptors in cancer by a new optimized ligand. *ChemMedChem*. 2011;6:1789-1791.
7. Herrmann K, Lapa C, Wester HJ, et al. Biodistribution and radiation dosimetry for the chemokine receptor CXCR4-targeting probe 68Ga-pentixafor. *J Nucl Med*. 2015;56:410-416.
8. Lapa C, Schreder M, Schirbel A, et al. [(68)Ga]Pentixafor-PET/CT for imaging of chemokine receptor CXCR4 expression in multiple myeloma - Comparison to [(18)F]FDG and laboratory values. *Theranostics*. 2017;7:205-212.
9. Lapa C, Luckerath K, Rudelius M, et al. [68Ga]Pentixafor-PET/CT for imaging of chemokine receptor 4 expression in small cell lung cancer--initial experience. *Oncotarget*. 2016;7:9288-9295.
10. Derlin T, Jonigk D, Bauersachs J, Bengel FM. Molecular Imaging of Chemokine Receptor CXCR4 in Non-Small Cell Lung Cancer Using 68Ga-Pentixafor PET/CT: Comparison With 18F-FDG. *Clin Nucl Med*. 2016;41:e204-205.
11. Werner RA, Kircher S, Higuchi T, et al. CXCR4-Directed Imaging in Solid Tumors. *Front Oncol*. 2019;9:770.
12. Weich A, Werner RA, Buck AK, et al. CXCR4-Directed PET/CT in Patients with Newly Diagnosed Neuroendocrine Carcinomas. *Diagnostics (Basel)*. 2021;11.
13. Bluemel C, Hahner S, Heinze B, et al. Investigating the Chemokine Receptor 4 as Potential Theranostic Target in Adrenocortical Cancer Patients. *Clin Nucl Med*. 2017;42:e29-e34.

14. Zhou X, Dierks A, Kertels O, et al. 18F-FDG, 11C-Methionine, and 68Ga-Pentixafor PET/CT in Patients with Smoldering Multiple Myeloma: Imaging Pattern and Clinical Features. *Cancers (Basel)*. 2020;12.
15. Pan Q, Cao X, Luo Y, Li J, Feng J, Li F. Chemokine receptor-4 targeted PET/CT with (68)Ga-Pentixafor in assessment of newly diagnosed multiple myeloma: comparison to (18)F-FDG PET/CT. *Eur J Nucl Med Mol Imaging*. 2020;47:537-546.
16. Herrmann K, Schottelius M, Lapa C, et al. First-in-Human Experience of CXCR4-Directed Endoradiotherapy with 177Lu- and 90Y-Labeled Pentixather in Advanced-Stage Multiple Myeloma with Extensive Intra- and Extramedullary Disease. *J Nucl Med*. 2016;57:248-251.
17. Lapa C, Hanscheid H, Kircher M, et al. Feasibility of CXCR4-Directed Radioligand Therapy in Advanced Diffuse Large B-Cell Lymphoma. *J Nucl Med*. 2019;60:60-64.
18. Maurer S, Herhaus P, Lippenmeyer R, et al. Side Effects of CXC-Chemokine Receptor 4-Directed Endoradiotherapy with Pentixather Before Hematopoietic Stem Cell Transplantation. *J Nucl Med*. 2019;60:1399-1405.
19. Keller T, Lopez-Picon FR, Krzyczmonik A, et al. Comparison of high and low molar activity TSPO tracer [(18)F]F-DPA in a mouse model of Alzheimer's disease. *J Cereb Blood Flow Metab*. 2020;40:1012-1020.
20. Lapa C, Kircher S, Schirbel A, et al. Targeting CXCR4 with [(68)Ga]Pentixafor: a suitable theranostic approach in pleural mesothelioma? *Oncotarget*. 2017;8:96732-96737.
21. Lewis R, Habringer S, Kircher M, et al. Investigation of spleen CXCR4 expression by [(68)Ga]Pentixafor PET in a cohort of 145 solid cancer patients. *EJNMMI Res*. 2021;11:77.
22. Kraus S, Dierks A, Rasche L, et al. (68)Ga-Pentixafor-PET/CT imaging represents a novel approach to detect chemokine receptor CXCR4 expression in myeloproliferative neoplasms. *J Nucl Med*. 2021.
23. Werner RA, Weich A, Higuchi T, et al. Imaging of Chemokine Receptor 4 Expression in Neuroendocrine Tumors - a Triple Tracer Comparative Approach. *Theranostics*. 2017;7:1489-1498.
24. Philipp-Abbrederis K, Herrmann K, Knop S, et al. In vivo molecular imaging of chemokine receptor CXCR4 expression in patients with advanced multiple myeloma. *EMBO Mol Med*. 2015;7:477-487.
25. Habringer S, Lapa C, Herhaus P, et al. Dual Targeting of Acute Leukemia and Supporting Niche by CXCR4-Directed Theranostics. *Theranostics*. 2018;8:369-383.
26. Duell J, Krummenast F, Schirbel A, et al. Improved Primary Staging of Marginal-Zone Lymphoma by Addition of CXCR4-Directed PET/CT. *J Nucl Med*. 2021;62:1415-1421.

27. Lapa C, Herrmann K, Schirbel A, et al. CXCR4-directed endoradiotherapy induces high response rates in extramedullary relapsed Multiple Myeloma. *Theranostics*. 2017;7:1589-1597.
28. Li X, Heber D, Leike T, et al. [68Ga]Pentixafor-PET/MRI for the detection of Chemokine receptor 4 expression in atherosclerotic plaques. *Eur J Nucl Med Mol Imaging*. 2018;45:558-566.
29. Vag T, Gerngross C, Herhaus P, et al. First experience with chemokine receptor CXCR4-targeted PET imaging of patients with solid cancers. *J Nucl Med*. 2016;57:741-746.
30. Demmer O, Dijkgraaf I, Schumacher U, et al. Design, synthesis, and functionalization of dimeric peptides targeting chemokine receptor CXCR4. *J Med Chem*. 2011;54:7648-7662.
31. Osl T, Schmidt A, Schwaiger M, Schottelius M, Wester HJ. A new class of PentixaFor- and PentixaTher-based theranostic agents with enhanced CXCR4-targeting efficiency. *Theranostics*. 2020;10:8264-8280.
32. Burger JA, Peled A. CXCR4 antagonists: targeting the microenvironment in leukemia and other cancers. *Leukemia*. 2009;23:43-52.
33. Zhao H, Guo L, Zhao H, Zhao J, Weng H, Zhao B. CXCR4 over-expression and survival in cancer: a system review and meta-analysis. *Oncotarget*. 2015;6:5022-5040.
34. Ghobrial IM, Liu CJ, Zavidij O, et al. Phase I/II trial of the CXCR4 inhibitor plerixafor in combination with bortezomib as a chemosensitization strategy in relapsed/refractory multiple myeloma. *Am J Hematol*. 2019;94:1244-1253.
35. Ludwig H, Weisel K, Petrucci MT, et al. Olaptosed pegol, an anti-CXCL12/SDF-1 Spiegelmer, alone and with bortezomib-dexamethasone in relapsed/refractory multiple myeloma: a Phase IIa Study. *Leukemia*. 2017;31:997-1000.
36. Galsky MD, Vogelzang NJ, Conkling P, et al. A phase I trial of LY2510924, a CXCR4 peptide antagonist, in patients with advanced cancer. *Clin Cancer Res*. 2014;20:3581-3588.

Graphical Abstract



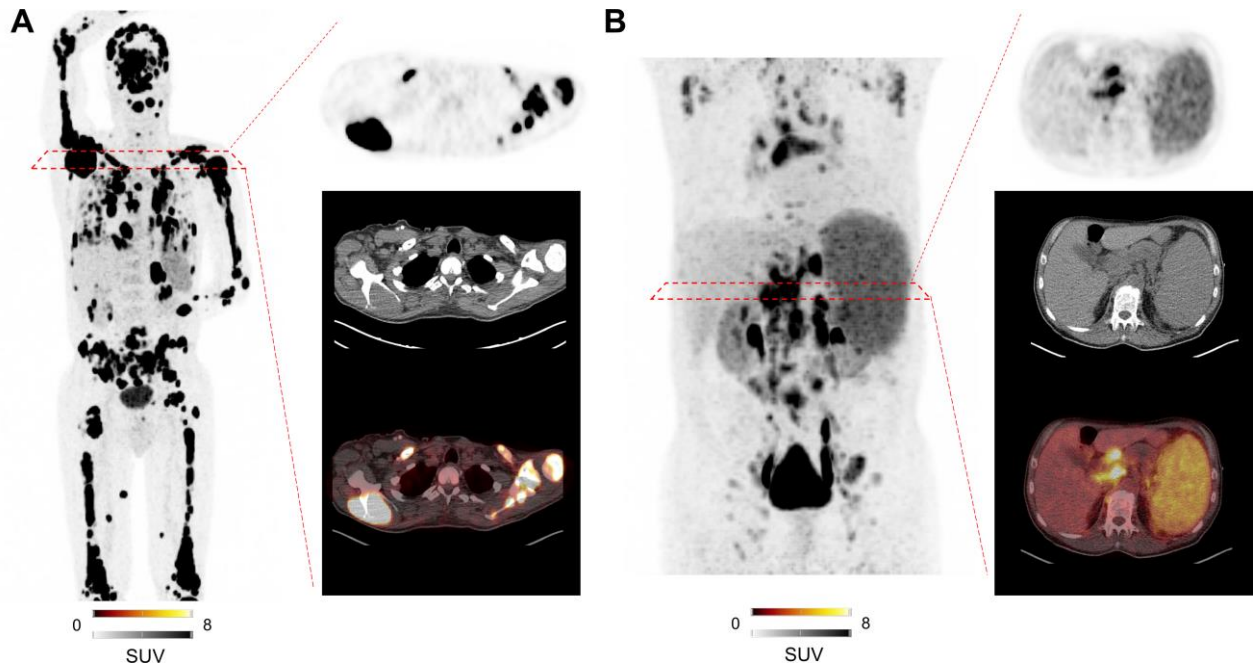


Figure 1. Maximum intensity projections of patients with hematologic malignancies imaged with CXCR4-directed ^{68}Ga -PentixaFor. The target lesion is also displayed on transaxial PET, CT, and PET/CT. Patient diagnosed with multiple myeloma (A; SUV_{max} in the target lesion: 74.3) and mantle cell lymphoma (B; SUV_{max} in the target lesion: 17.2). Substantially low background activity allowed for precise determination of disease sites.

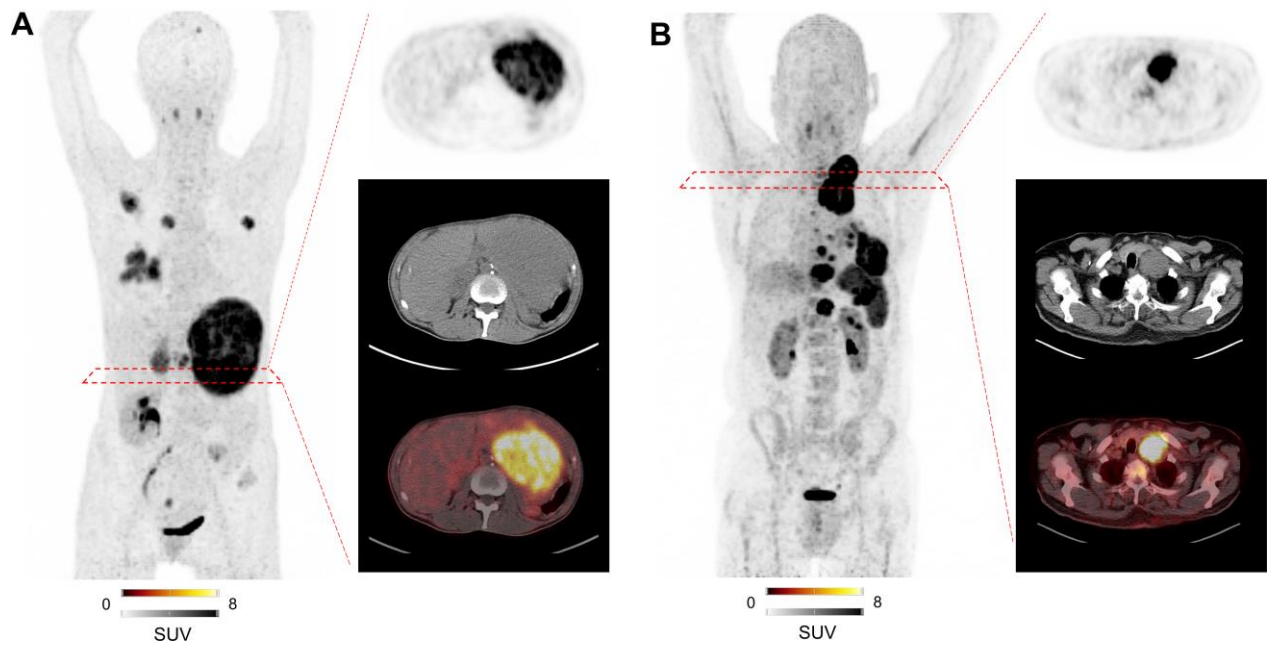


Figure 2. Maximum intensity projections of patients with solid tumor entities imaged with CXCR4-directed ^{68}Ga -PentixaFor. Target lesion is also displayed on transaxial PET, CT, and PET/CT. Patient diagnosed with adrenocortical carcinoma (A; SUV_{max} in the target lesion: 13.2) and small cell lung carcinoma (B; SUV_{max} in the target lesion: 19.4). Background activity was substantially low, providing a precise read-out of disease sites.

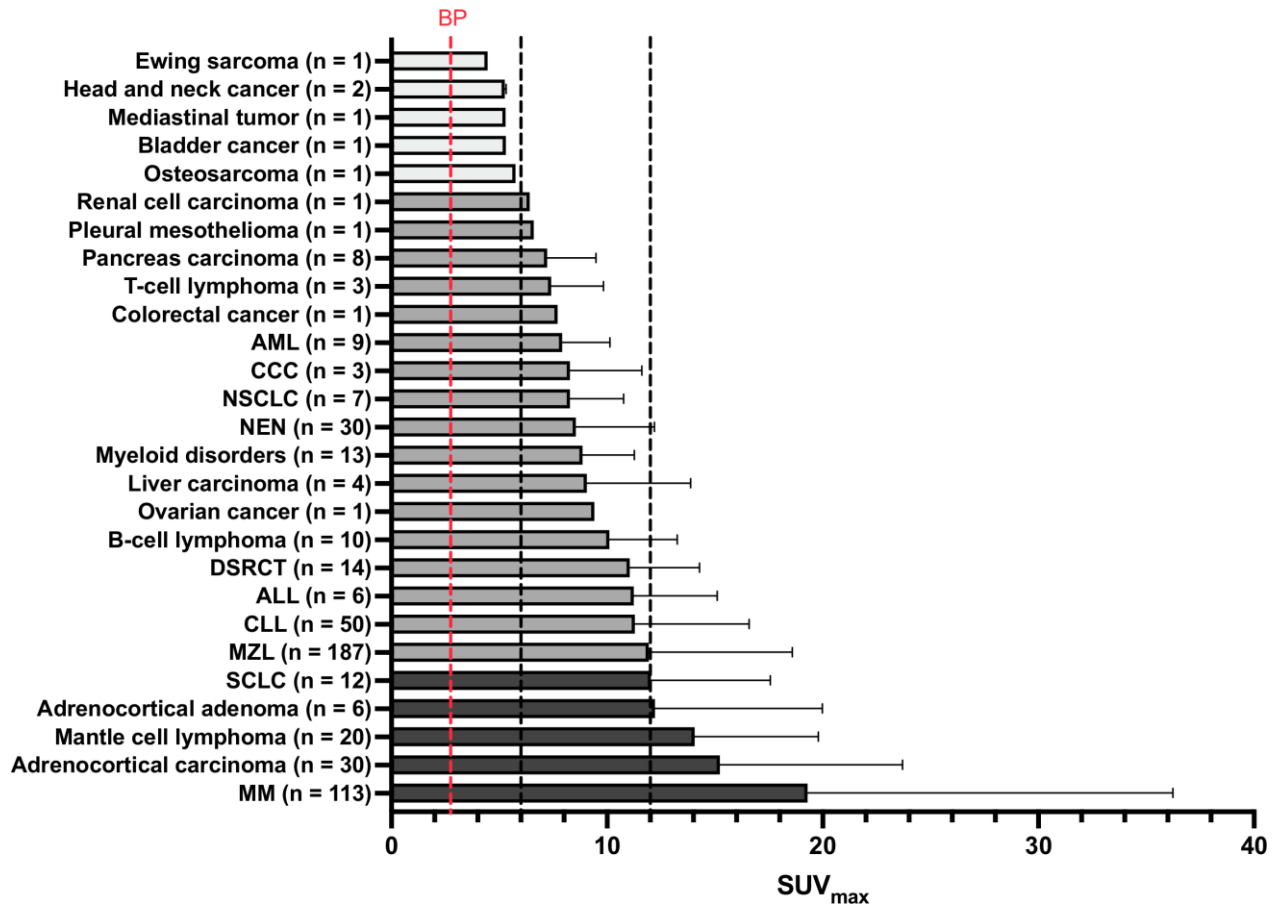


Figure 3. Bar chart displaying average SUV_{max}. Mean ± SD is indicated. Black dotted lines show SUV_{max} cutoffs of 6 and 12, respectively. BP = Blood pool (red dotted line). AML = acute myeloid leukemia. CCC = cholangiocarcinoma. NSCLC = non-small cell lung carcinoma. NEN = neuroendocrine neoplasm. DSRCT = Desmoplastic Small Round Cell Tumor. ALL = acute lymphoblastoid leukemia. CLL = chronic lymphocytic leukemia. MZL = marginal zone lymphoma. SCLC = small cell lung carcinoma. MM = multiple myeloma. In individual lesions, a markedly increased SUV_{max} of up to 85.8 was observed. Number of investigated patients (n) per diagnosis group is given in parentheses.

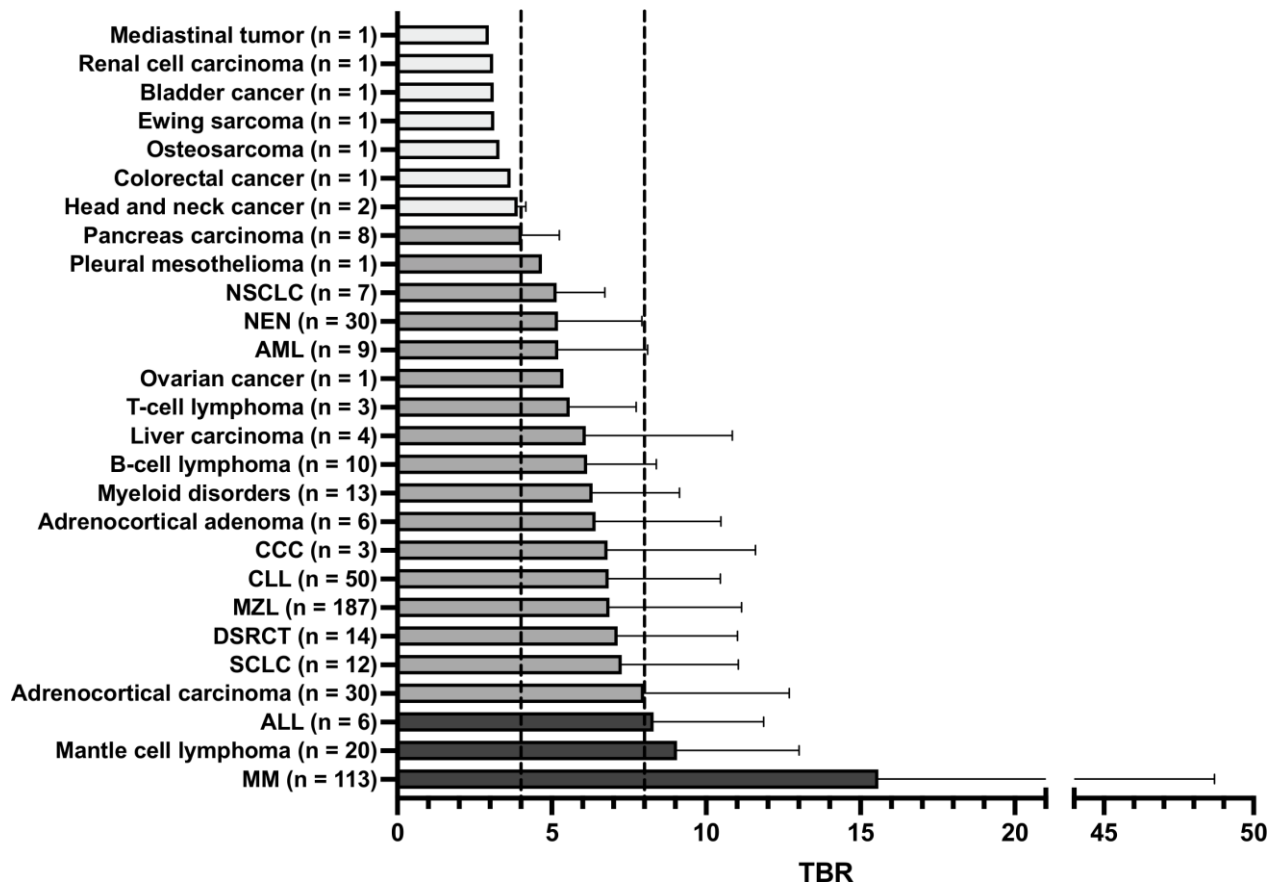


Figure 4. Bar chart displaying average TBR. Mean \pm SD is indicated. Black dotted lines show TBR cutoffs of 4 and 8, respectively. NSCLC = non-small cell lung carcinoma. NEN = neuroendocrine neoplasm. AML = acute myeloid leukemia. CCC = cholangiocarcinoma. CLL = chronic lymphocytic leukemia. MZL = marginal zone lymphoma. DSRCT = Desmoplastic Small Round Cell Tumor. SCLC = small cell lung carcinoma. ALL = acute lymphoblastoid leukemia. MM = multiple myeloma. Number of investigated patients (n) per diagnosis group is given in parentheses.

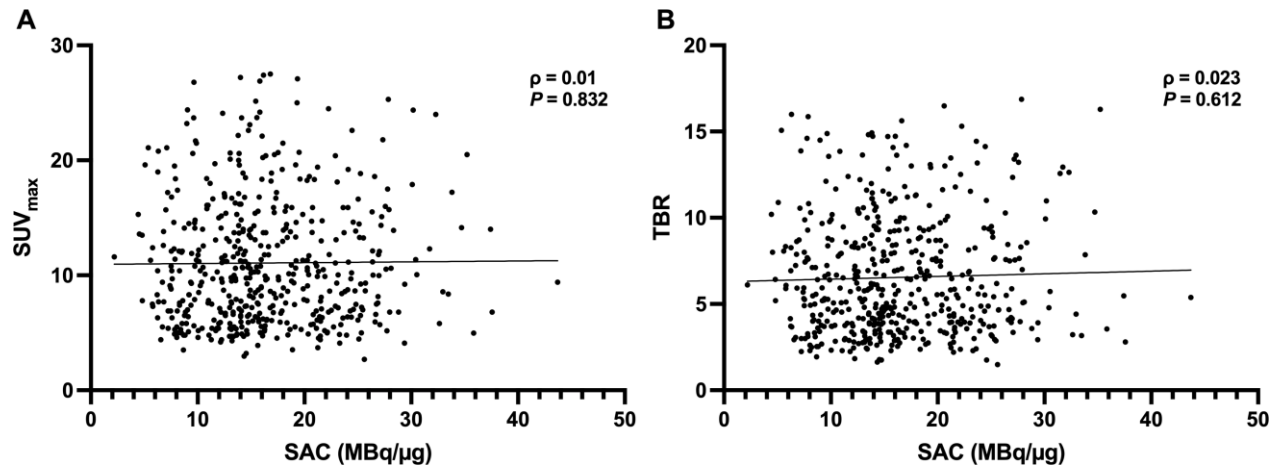
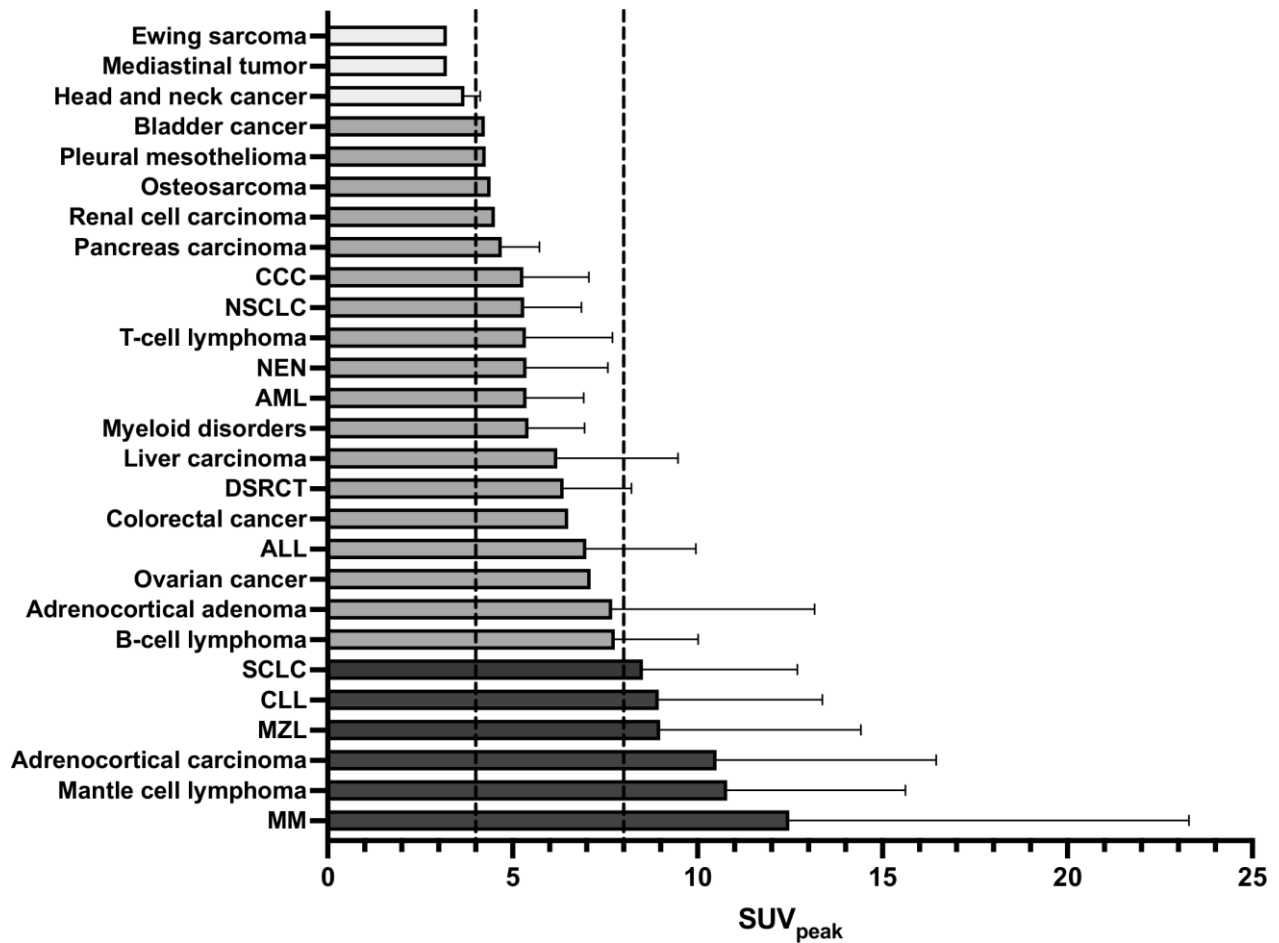


Figure 5. Correlation plots between specific activity in MBq/μg and (A) SUV_{max} and (B) TBR. Significant Spearman's Rho (ρ) and P are displayed. No significance was reached.

Diagnosis	Number of Scans
Marginal zone lymphoma	187 (35)
Multiple myeloma	113 (21.1)
Chronic lymphocytic leukemia	50 (9.3)
Adrenocortical carcinoma	30 (5.6)
Neuroendocrine neoplasm	30 (5.6)
Mantle cell lymphoma	20 (3.7)
Desmoplastic Small Round Cell Tumor	14 (2.6)
Myeloid disorders	13 (2.4)
Small Cell Lung Carcinoma	12 (2.2)
B-cell lymphoma	10 (1.9)
Acute myeloid leukemia	9 (1.7)
Pancreas carcinoma	8 (1.5)
Non-Small Cell Lung Carcinoma	7 (1.3)
Adrenocortical adenoma	6 (1.1)
Acute lymphoblastoid leukemia	6 (1.1)
Liver Carcinoma	4 (0.7)
T-cell lymphoma	3 (0.6)
Cholangiocarcinoma	3 (0.6)
Head and neck cancer	2 (0.4)
Colorectal cancer	1 (0.2)
Pleural mesothelioma	1 (0.2)
Renal cell carcinoma	1 (0.2)
Ovarian cancer	1 (0.2)
Ewing sarcoma	1 (0.2)
Osteosarcoma	1 (0.2)
Mediastinal tumor*	1 (0.2)
Bladder cancer	1 (0.2)

Table 1. Overview of positive ⁶⁸Ga-PentixaFor PET-scans and individual diagnoses of patients included. Percentages are given in parentheses. *not otherwise specified.



Supplemental Figure 1. Bar chart displaying average SUV_{peak}. Mean ± SD is indicated. Black dotted lines show SUV_{peak} cutoffs of 4 and 8, respectively. CCC = cholangiocarcinoma. NSCLC = non-small cell lung carcinoma. NEN = neuroendocrine neoplasm. AML = acute myeloid leukemia. DSRCT = Desmoplastic Small Round Cell Tumor. ALL = acute lymphoblastoid leukemia. SCLC = small cell lung carcinoma. CLL = chronic lymphocytic leukemia. MZL = marginal zone lymphoma. MM = multiple myeloma.